Published in final edited form as:
Exp Eye Res. 2009 March ; 88(3): 467–478. doi:10.1016/j.exer.2008.10.023.

Transduced viral IL-10 is exocytosed from lacrimal acinar secretory vesicles in a myosin-dependent manner in response to carbachol

Jiansong Xie[a], **Ronald R. Marchelletta**[a], **Padmaja B. Thomas**[b,c], **Damon T. Jacobs**[d], **Francie A. Yarber**[a], **Richard E. Cheney**[d], **Sarah F. Hamm-Alvarez**[a,b], and **Melvin D. Trousdale**[b,c,*]

a *Department of Pharmacology and Pharmaceutical Sciences, University of Southern California, USA*

b *Department of Ophthalmology, University of Southern California, USA*

c *Doheny Eye Institute, University of Southern California, USA*

d *Department of Cell and Molecular Physiology, University of North Carolina, USA*

Abstract

The purpose of this study was to determine the intracellular trafficking and release pathways for the therapeutic protein, viral IL-10 (vIL-10), from transduced acinar epithelial cells from rabbit lacrimal gland. Primary cultured rabbit lacrimal gland acinar cells (LGACs) were transduced with adenovirus serotype 5 containing viral interleukin-10 (AdvIL-10). The distribution of vIL-10 was assessed by confocal fluorescence microscopy. Carbachol (CCH)-stimulated release of vIL-10 was quantified by ELISA. vIL-10 localization and exocytosis was probed in response to treatments with agents modulating actin- and myosin-based transport. vIL-10 immunoreactivity was detected in large intracellular vesicles in transduced LGAC. vIL-10 was partially co-localized with biosynthetic but not endosomal compartment markers. vIL-10 release was sensitive to CCH, and the kinetics of release showed an initial burst phase that was similar but not identical to that of the secretory protein, β-hexosaminidase. Disassembly of actin filaments with latrunculin B significantly increased CCH-stimulated vIL-10 secretion, suggesting that vIL-10 was released from stores sequestered beneath the subapical actin barrier. That release required the activity of actin-dependent myosin motors previously implicated in secretory vesicle exocytosis was confirmed by findings that CCH-stimulated vIL-10 release was reduced by inhibition of non-muscle myosin 2 and myosin 5c function, using ML-7 and overexpression of dominant negative myosin 5c, respectively. These results suggest that the majority of vIL-10 transgene product is packaged into a subpopulation of secretory vesicles that utilize actin-dependent myosin motors for aspects of actin coat assembly, compound fusion and exocytosis at the apical plasma membrane in response to CCH stimulation.

Keywords

lacrimal gland; ocular surface; gene therapy; cytokines; interleukin-10; myosin; Myo5c

1. Introduction

A common cause of ocular morbidity in developed countries is keratoconjunctivitis sicca (KCS) or “dry eye”. KCS due to lacrimal insufficiency is termed tear-deficient KCS, and this

* Correspondence to: Melvin D. Trousdale, Doheny Eye Institute, USC Keck School of Medicine, 1450 San Pablo Street, DVRC 204, Los Angeles, CA 90033, USA. Tel.: +1 323 442 6610; fax: +1 323 442 6688. *E-mail address*: mtrousdale@doheny.org (M.D. Trousdale)..

form of KCS affects tens of millions of people around the world (Schaumberg et al., 2003). Tear-deficient KCS can be a consequence of the autoimmune disease, Sjögren's syndrome (SjS), affecting 1−5 million Americans each year, or occur through SjS-independent mechanisms (Mircheff et al., 2005; Lemp, 2005; Zoukhri, 2006). SjS is characterized by lymphocytic infiltration of the lacrimal and salivary glands. These cellular infiltrates produce pro-inflammatory cytokines that cause severe functional impairment of the glands leading to dry eyes (i.e. KCS) and dry mouth (i.e. xerostomia) (Mircheff et al., 2005; Lemp, 2005; Zoukhri, 2006). SjS and other forms of tear-deficient KCS cause major problems for the ocular surface, particularly the cornea, which relies upon tear proteins as nutrients, anti-infectives and growth factors (Pflugfelder et al., 2000). Treatment regimens are currently inadequate and are focused on easing of symptoms rather than treatment of the underlying disease (Fox, 2000).

The hallmark histopathological feature of SjS is the appearance of focal, periductal and perivascular lymphocytic infiltrates in the lacrimal and salivary glands, and this decreases the gland's ability to produce fluid and protein. Effector CD4+ cells and regulatory CD8+ T lymphocytes are the most common immune cells in these infiltrates, with CD4+ cells being most prominent with a ratio of 4:1 compared to CD8+ cells in autoimmune-diseased glands. In normal lacrimal glands, regulatory CD8+ cells are more common, at a ratio of 2:1, CD8 to CD4 (Segerberg-Konttinen, 1988; Zhu et al., 2003b).

Gene therapy provides an opportunity for treating many different diseases (Crystal, 1995; Lever and Goodfellow, 1995; Goldfine et al., 1997), including autoimmune diseases (Zhu et al., 2003b; Mathisen and Tuohy, 1998; Evans et al., 1998; Seroogy and Fathman, 1998). Using a rabbit model of induced autoimmune dacryoadenitis that mimics SjS (Zhu et al., 2003a), we previously demonstrated in a prophylactic study that adenovirus-mediated transduction of lacrimal gland acinar cells with either the anti-inflammatory cytokine gene, viral interleukin-10 (vIL-10) or the soluble tumor necrosis factor, (TNF)-α inhibitor, resulted in the appearance of transgene products in tears combined with the reduction of clinical and immunopathologic manifestations (Zhu et al., 2003b). Later, in a therapeutic study using the same animal model, we reported that the expression of an anti-inflammatory cytokine gene in the lacrimal gland promoted recovery of tear production and tear stability while reducing immunopathology in rabbit lacrimal glands with induced autoimmune dacryoadenitis (Trousdale et al., 2005). From these studies, it was concluded that therapeutic levels of the anti-inflammatory gene product were achieved in the lacrimal gland as well as on the corneal surface. These results raised the question of whether the therapeutic transgene product exits the transduced acinar cell via its apical or basolateral membrane or both. The purpose of this study was to determine the intracellular trafficking and release pathway(s) of transduced vIL-10.

The lacrimal gland acinar cell (LGAC) is a secretory epithelial cell that comprises the major cell type within the lacrimal gland. These cells are organized into acini, with adjacent apical membrane domains surrounding a lumen (Scheme 1); fluid and proteins released at the apical plasma membrane drain from the lumen through a series of ducts onto the ocular surface. Some apical secretion of proteins into tear fluid by the lacrimal gland occurs at a constitutive level, while additional apical release of tear proteins from secretory vesicles by fusion at the apical plasma membrane is accelerated considerably by exposure to secretagogues. In situ physiological stimulation occurs in response to the release of agonists from innervating sympathetic and parasympathetic neurons; the actions of the physiological agonist, acetylcholine, are mimicked in our in vitro study by the muscarinic agonist, carbachol (CCH).

Tear proteins destined for apical release from the lacrimal gland are stored in the LGAC within a variety of secretory vesicles (SV), which can be detected by electron microscopy as a heterogeneous population of serous and mucous vesicles sized ~0.5−1 μM (da Costa et al., 2006; Jerdeva et al., 2005a; Marchelletta et al., 2008). Some of the effectors that govern

exocytosis of these SV at the apical plasma membrane have been identified, while others remain to be established (Wu et al., 2006). Briefly, lacrimal gland SV are enriched in specific proteins which provide targeting specificity, including Rab proteins, small GTPases specific for donor membrane compartments, and SNARE proteins which enable the formation of a fusion pore between donor and acceptor membranes. In addition to these effector proteins, additional factors contribute to SV formation, maturation and exocytosis including cytoskeletal filaments (actin and microtubules) and their associated motor proteins.

Actin filaments and microtubules exist in all eukaryotic cells, and have been implicated in diverse steps in vesicular transport. Both polymers provide paths which support the transport of membrane cargo driven by different types of motor proteins. The ability of actin filaments to be rapidly remodeled in response to cellular cues as well as to be utilized for generation of contractile functions is also key in its activities in membrane trafficking. Actin filaments play an important role in the terminal exocytosis of SV located beneath the apical plasma membrane in LGAC. Specifically, disassembly of the subapical actin network occurs in stimulated acini, facilitating access of the activated SV to the apical plasma membrane. Coincident with this disassembly, a network of basketlike actin filaments assembles around the base of the fusing SV, facilitating compound fusion prior to the contact of the vesicular aggregate with the apical membrane. The actin network also participates in movement of the fusion intermediate towards the apical plasma membrane, which is now more accessible due to the local actin disassembly (Jerdeva et al., 2005a,b; Wu et al., 2006). The contraction of actin filaments in retraction of the actin-coated fusion intermediate to the apical plasma membrane is known to utilize non-muscle myosin 2 (Myo2) (Jerdeva et al., 2005a). Another actin-based motor protein, the unconventional myosin motor, myosin 5c (Myo5c), is also enriched on SV and is an established SV marker (Marchelletta et al., 2008). We have recently shown that Myo5c also participates in aspects of actin coat formation, SV compound fusion and content extrusion (Marchelletta et al., 2008).

Generally, microtubule-based vesicular transport occurs over relatively long distances in cytoplasm. Our work in LGAC has implicated microtubules and the microtubule-based motor, cytoplasmic dynein, in the formation and movement of a population of recruitable secretory vesicles (rSV) from the cell interior towards the apical membrane, to sustain the secretory response after the initial burst of release from SV already localized in the subapical cytoplasm (Wang et al., 2003). A schematic of the key processes involved in movement and release of apically-targeted SV and the roles of microtubules and actin filaments is shown in Scheme 1.

Exocytosis of vesicles can also occur at the basolateral membrane of LGAC, although the molecular mechanisms are not well established. However, functional studies do not suggest the same dependence on cytoskeletal filaments as at the apical membrane in secretory epithelia. Additionally, there is little evidence for the existence of a pool of pre-formed vesicles which serve as a source of secretory proteins that are released immediately upon cell stimulation, leading to the burst phenomenon as seen for apically-released secretory products.

To begin to elucidate the mechanisms of transduced vIL-10 sorting and release from LGAC, we have examined its localization within cultured LGAC, its release kinetics in response to CCH stimulation, and the sensitivity of release to agents which influence actin- and myosin-dependent secretory processes. Our results suggest that the majority of vIL-10 is routed through the apical secretory pathway where it is sequestered in a subpopulation of SV and released in a process that involves actin filaments and myosin motors.

2. Methods

2.1. Reagents

Carbachol (CCH), rhodamine-phalloidin and goat anti-rabbit secondary antibody conjugated to FITC were purchased from Sigma–Aldrich (St. Louis, MO). Rat monoclonal antibody to IL-10 and BD OptEIA™ human IL-10 ELISA kit II were purchased from BD Biosciences Pharmingen (San Diego, CA). Goat polyclonal antibody to early endosomal antigen 1 (EEA1) and FITC-conjugated chicken anti-rat IgG were purchased from Santa Cruz Biotechnology (Santa Cruz, CA). Mouse monoclonal antibody to γ-adaptin was purchased from Transduction Laboratories (Lexington, KY). Rabbit polyclonal antibody to Myo5c was raised against a His-tagged protein fused to human Myo5c tail as described previously (Rodriguez and Cheney, 2002). Latrunculin B (LAT) and the myosin light chain kinase inhibitor, ML-7 [1-(5-Iodonaphthalene-1-sulfonyl)homopiperazine, HCl], were purchased from EMD Biosciences (San Diego, CA). Matrigel was obtained from Collaborative Biochemicals (Bedford, MA). ProLong antifade mounting media, Alexa Fluor® 568-conjugated goat anti-rat IgG, Alexa Fluor® 488 donkey anti-goat IgG, Alexa Fluor® 488 goat anti-mouse IgG1 (γ1), Alexa Fluor® 680 goat anti-rat IgG, Alexa Fluor® 647 phalloidin and 4′, 6-diamidino-2-phenylindole (DAPI) were from Molecular Probes/Invitrogen (Eugene, OR). Paraformaldehyde was purchased from Polysciences (Warrington, PA). Cell culture reagents were obtained from Life-Technologies. All other chemicals were reagent grade and obtained from standard suppliers.

2.2. Cell isolation and culture

All animal work was performed in accordance with the Guiding Principles for Use of Animals in Research. Female New Zealand white rabbits weighing between 1.8 and 2.2 kg were obtained from Irish Farms (Norco, CA). LGACs were isolated and maintained in a laminin-based primary culture system for 2−3 days as described previously (Gierow et al., 1995; Hamm-Alvarez et al., 1997; da Costa et al., 1998). These culture conditions resulted in reconstitution of epithelial polarity, establishment of acinar lumena, and formation of SV (Scheme 1) (Gierow et al., 1995; Hamm-Alvarez et al., 1997; da Costa et al., 1998, 2003; Wang et al., 2003; Xie et al., 2004a,b, 2006; Jerdeva et al., 2005a,b).

2.3. Generation of adenoviral vectors

Replication-defective adenovirus serotype 5 (Ad) containing the Epstein Barr virus IL-10 gene (AdvIL-10) and the green fluorescent protein (GFP) reporter gene (Ad-GFP) were constructed as described previously (Zhu et al., 2002; Wang et al., 2004; Jerdeva et al., 2005a). Replication-defective Ad5 containing the GFP-fused tail region (amino acid residues 902−1742) of Myo5c (Ad-Myo5c-tail-GFP) was constructed using the AdenoX expression kit 1 (Clontech) as described previously (Marchelletta et al., 2008).

2.4. Confocal fluorescence microscopy

Rabbit primary LGACs were seeded onto Matrigel-coated 18 mm circular glass coverslips in 12-well plates at 2×10^6 cells/well. On day 2 of culture, reconstituted acini were transduced with AdvIL-10 at a MOI of 5 for 24 h. Cells were rinsed with Dulbecco's phosphate buffered saline (DPBS), then fixed with 4% paraformaldehyde and permeabilized with 0.1% Triton X-100 as previously described (da Costa et al., 1998, 2003; Zhang et al., 2000; Wang et al., 2003; Jerdeva et al., 2005b) and the distribution of vIL-10 and that of other compartment markers was assessed by confocal fluorescence microscopy using a rat anti-human IL-10 monoclonal antibody and other primary and secondary fluorophore-conjugated antibodies or fluorescent probes. Confocal images were obtained with a Zeiss LSM 510 Meta NLO imaging system equipped with Argon, red HeNe and green HeNe lasers and a Coherent Chameleon Ti-

sapphire tunable multiphoton laser mounted on a vibration-free table. Panels were compiled in Adobe Photoshop 7.0 (Adobe Systems Inc., Mountain View, CA).

In some experiments, Ad IL-10 (1×10^8 PFU in 0.2 mL) was injected into each rabbit's inferior lacrimal gland using a 25-gauge butterfly needle on a tuberculin syringe. To avoid tissue damage caused by rapid volume expansion, the microvolume delivery system was set to deliver 10 μL at 10 s intervals (10 μL × 20 repetitions 200 μL). Rabbits were sacrificed by injection of pentobarbital sodium (56 mg/kg) 5 days after inoculation. The inferior lacrimal glands of the injected eyes were removed from each animal and dissected longitudinally into two parts and each part was embedded in optimal cutting temperature (OCT) compound (Miles, Inc., Elkhart, IN) after fixing in 4% paraformaldehyde and sucrose rehydration. Cryosections were used and immunohistologic staining was performed as previously described (Zhu et al., 2004; da Costa et al., 2006).

2.5. Secretion assays

Secretion assays were based on those described previously (da Costa et al., 1998; Zhang et al., 2000; Wang et al., 2003). Rabbit LGACs were seeded onto Matrigel-coated 24-well plates at 1×10^6 cells/well. On day 2 of culture, reconstituted acini were transduced with AdvIL-10 at a MOI of 5 for 24 h. Control and transduced acini were then incubated in fresh medium for 1 h to allow cell equilibration. In some cases, cells were treated with LAT (10 μM, 60 min) or ML-7 (40 μM, 15 min). After treatment with or without CCH (1−1000 μM, 0−180 min), aliquots of the medium were removed for measurement of vIL-10 content or β-hexosaminidase activity. The amounts of vIL-10 or β-hexosaminidase present under each condition were calculated from three replicate wells/treatment in each assay, and values normalized to total cellular protein before comparison across treatments using Student's *t*-test with the criterion for significance at $p \leq 0.05$ as previously described (Hamm-Alvarez et al., 2003; Wang et al., 2004). It should be noted that the lumenal regions in the reconstituted cultures are accessible to culture medium (Jerdeva et al., 2005b), so that apically-released proteins can be measured in the medium. In these cultures, we are unfortunately unable to distinguish between apical and basolateral release of proteins in unstimulated LGAC, but the large bolus due to CCH stimulation is due to apical exocytosis.

For measurement of vIL-10 release, aliquots of medium were diluted and vIL-10 concentrations were quantified on 96-well plates using BD OptEIA™ human IL-10 ELISA kit II (BD Biosciences Pharmingen, San Diego, CA). The procedures were performed according to the manufacturer's recommended protocol and concentrations determined from the standard curve. β-Hexosaminidase activity was assessed on 96-well plates using methylumbelliferyl-D-glucosaminide as substrate. Protein contents were determined on 96-well plates using the Micro BCA Protein Assay (Pierce) with bovine serum albumin as standard. A Tecan GENios Plus UV/Visible/fluorescence plate reader (Phenix Research Products, Hayward, CA, USA) was used to measure reaction products. In some experiments, LGACs transduced with Ad-Myo5c-tail-GFP or Ad-GFP in addition to AdvIL-10 were processed as above to measure release of vIL-10.

3. Results

3.1. vIL-10 immunoreactivity is detected in large intracellular vesicles in transduced LGAC

To determine the intracellular trafficking and release pathways of vIL-10, we first assessed the intracellular distribution of vIL-10 transgene product in reconstituted LGAC transduced with AdvIL-10 by confocal fluorescence microscopy. As shown in Fig. 1, under our culture conditions individual acinar cells reassociate to form acinus-like structures organized around the lumen, the secretory domain that can be identified by the intense labeling due to the

subapical actin filament network (da Costa et al., 1998). The nuclei are localized towards the basolateral membranes. vIL-10 immunoreactivity was detected within apparent vesicles in resting acini transduced with AdvIL-10; it accumulated primarily in large (0.5−1 μm) vesicles as estimated using the Ruler Tool within the Zeiss LSM software. This labeling was largely detected just beneath the lumenal regions. Some intracellular labeling associated with vIL-10 could also be detected adjacent to the basolateral plasma membrane (Fig. 1A). No immunofluorescent signal could be recovered in control (nontransduced) cells (data not shown).

To show that the intracellular distribution of vIL-10 transgene product we observed in the transduced primary LGAC culture system used, was comparable to that detected in intact tissue, we used AdvIL-10 to inject intact rabbit lacrimal gland and examined the distribution of vIL-10 transgene product in transduced lacrimal gland tissue. As shown in Fig. 1B, consistent with the in vitro result, vIL-10 immunoreactivity was detected in vesicle-like structures beneath the apical plasma membranes in transduced lacrimal gland tissue.

In this and subsequent experiments, it should be noted that our confocal fluorescence microscopy analysis detected strong vIL-10 immunofluorescence in about 20−30% of cells, suggesting a lower transduction efficiency with this vector than with other Ad5-derived vectors reported previously in LGAC (Wang et al., 2003, 2004; Jerdeva et al., 2005a,b).

3.2. vIL-10 is partially co-localized with biosynthetic but not endosomal markers

We examined the extent of co-localization of vIL-10 with biosynthetic membranes' compartments (i.e. the Golgi complex and trans-Golgi network) which are responsible for producing and packaging vesicles containing secretory proteins that are targeted either to the apical or basolateral plasma membranes. As expected, in resting cells transduced with AdvIL-10, vIL-10 was partially co-localized with the trans-Golgi network marker, γ-adaptin (Fig. 2A). A lesser degree of co-localization was observed with the Golgi marker, Rab6 (data not shown).

Since biosynthetic compartments communicate with apically and basolaterally-targeted exocytotic pathways, and basolateral release to the interstitium of the lacrimal gland was one potential route of secretory protein release, we examined the co-localization of vIL-10 with membrane trafficking proteins associated with basolateral endosomes which accommodate the transit of some basolaterally-targeted secretory products. As shown in Fig. 2B, in resting cells transduced with AdvIL-10, there was no co-localization of vIL-10 with the early endosome marker, EEA1. There was also no co-localization of vIL-10 with the recycling endosome marker, Rab4, or the early endosome marker Rab5a (data not shown). These findings suggest that vIL-10 is not extensively enriched in trafficking pathways in communication with the basolateral membranes, although they do not exclude the possibility that some vIL-10-enriched vesicles may be able to transit directly from Golgi and trans-Golgi sorting compartments and fuse at the basolateral membranes.

We had difficulty assessing the co-localization of vIL-10 with markers of mature apically-targeted SV, since the fixation conditions that resulted in optimal resolution of these markers (Rab3D and Myo5c) were not compatible with the fixation conditions that yielded strong vIL-10 immunofluorescence. The possibility that vIL-10 was packaged in apically-targeted SV, consistent with its observed enrichment in large vesicles adjacent to the actin-enriched lumena (Fig. 1), was subsequently explored from a functional standpoint as well as using co-transduction with an SV marker, Myo5c for confocal fluorescence microscopy.

3.3. vIL-10 release from LGAC is increased by CCH stimulation

To determine how vIL-10 secretion from LGAC responded to secretagogue stimulation, basal and carbachol (CCH)-stimulated release of vIL-10 was measured from LGAC using ELISA and biochemical assays, respectively. The secretory product, β-hexosaminidase (da Costa et al., 1998; Andersson et al., 2006) was measured under the same conditions, for comparison. In order to determine the optimal dose for further studies on stimulated secretion, release of vIL-10 and β-hexosaminidase from LGAC was measured following exposure to 1 μM, 10 μM, 100 μM or 1 μM CCH for 30 min time interval. The dose dependence of CCH-stimulated release of vIL-10 and β-hexosaminidase is shown in Fig. 3. These experiments showed that transduced LGAC secreted vIL-10 at a low but detectable rate in the absence of CCH. CCH stimulation increased the secretion of both vIL-10 and β-hexosaminidase, showing a maximal effect at 100 μM and a supramaximal effect at 1 μM. The similar dose response of vIL-10 and β-hexosaminidase suggested that both cargo proteins were secreted largely by similar mechanisms. This observation is consistent with other measurements of the optimal CCH dose required for maximal stimulation in lacrimal acini (Gierow et al., 1995; da Costa et al., 2003).

We therefore chose to use the maximal CCH concentration (100 μM) to perform time course study of CCH-stimulated release of vIL-10 and β-hexosaminidase at time intervals from 0 to 180 min. As shown in Fig. 4, CCH stimulation significantly ($p \leq 0.05$) increased the secretory rate at all times measured (0−180 min). The curve appeared biphasic, with a robust and linear increase from 0 to 90 min, and a tapering response from 90 to 180 min. The sensitivity of the release to CCH and the rapid burst of release at early times (50% of the total product released was released within the first 30 min of the 180 min incubation period) suggested that a substantial portion of vIL-10 transgene product was directed into the acinar cells' regulated apical secretory pathway. This observation is also consistent with studies which previously have recovered vIL-10 in tears from the lacrimal glands of rabbits transduced with AdvIL-10 (Zhu et al., 2004).

3.4. Acute release of vIL-10 from LGAC

To further characterize the kinetics of vIL-10 release, the acute vIL-10 release profile was assessed. The time course of release of vIL-10 and β-hexosaminidase from control and transduced acini over 30 min without or with 100 μM CCH is summarized in Fig. 5. Fig. 5A shows the effect of 100 μM CCH on vIL-10 release; little vIL-10 was released within the first 5 min, but the onset of a rapid release at 10 min was detected that was essentially complete by 15 min. Little additional release occurred between 15 and 30 min. Fig. 5B shows the time course of release of β-hexosaminidase in parallel. β-Hexosaminidase shows an initial rapid phase of release (0−15 min), and a second flat phase of release (15−30 min). This latter profile is consistent with the rapid discharge of pre-formed SV followed by the sustained release from rSV, as suggested previously (Wang et al., 2003). These acute secretion experiments showed that the kinetics of release of vIL-10 are similar but not identical to that of secretory protein, β-hexosaminidase. Specifically, the burst of release characteristic of proteins in pre-formed SV is delayed slightly for vIL-10, suggesting that the bulk of this protein is in a CCH-sensitive pool of vesicles that can be rapidly but not immediately mobilized.

3.5. Disruption of actin filaments alters vIL-10 secretion from LGAC

We have previously shown that disassembly of actin microfilaments with latrunculin B (LAT) enhanced the CCH-stimulated release of bulk protein and the transduced SV marker, syncollin-GFP (Jerdeva et al., 2005a), likely due to removal of the actin filament network that normally prevents access of SV to the apical plasma membrane (Scheme 1). We have postulated that this response is due to the increased access of SV to the apical plasma membrane, once the dense subapical filament network is removed. To investigate the possible involvement of actin

filaments in vIL-10 secretion, we examined the effect of LAT on CCH-stimulated release of vIL-10 from control and transduced acini. For simplicity, we focused on 0 min, 30 min and 180 min time points. As shown in Fig. 6A, secretion experiments indicated that disassembly of actin filaments with LAT resulted in a small but significant enhancement of CCH-stimulated vIL-10 secretion at 30 min, a phenomenon very similar to the stimulatory effect of LAT on CCH-stimulated secretion of the specific SV marker, syncollin-GFP (Jerdeva et al., 2005a).

These data were further supported by confocal fluorescence microscopy. Consistent with the biochemical studies shown earlier (Figs. 3-5), acute CCH stimulation for 30 min reduced intracellular vIL-10 staining in untreated acini, especially the immunofluorescence signal adjacent to the apical plasma membrane (Fig. 6B). Confocal fluorescence microscopy also revealed that LAT pretreatment appeared to reduce intracellular vIL-10 staining in transduced cells stimulated with 100 μM CCH for 30 min, although it was not clear if the effect was more pronounced at the apical plasma membrane due to the extensive disruption of actin filament-associated structures caused by LAT (Fig. 6B). These results suggest that actin microfilaments may serve as a barrier in the regulated vIL-10 secretory pathway at the apical plasma membrane.

We have previously shown that the microtubule array and cytoplasmic dynein participate in apically-targeted transport of rSV (Wang et al., 2003), a response which aids in maintaining the secretory response following the immediate release of pre-formed SV. Parallel experiments using the microtubule-disrupting agent, nocodazole, revealed no evidence for a role for microtubules in CCH-stimulated release of vIL-10 (data not shown). These results suggest that the microtubule cytoskeleton does not play a critical role in acute vIL-10 secretion from LGAC.

3.6. Inhibition of myosin motors significantly reduces vIL-10 secretion

ML-7 has been utilized extensively as a selective inhibitor of myosin light chain kinase (Saitoh et al., 1987), leading to specific inhibition of non-muscle Myo2 activity. Our previous work has established that ML-7 treatment results in stabilization of actin-coated fusion intermediates in CCH-stimulated acini (Jerdeva et al., 2005a), likely due to impaired ability of Myo2 associated with the actin coat surrounding the fusing vesicles to exert force to promote SV compression and fusion. To test whether CCH-stimulated vIL-10 release was sensitive to ML-7, we pretreated LGAC with ML-7 prior to measurement of vIL-10 release without and with CCH. As shown in Fig. 7, ML-7 significantly reduced CCH-stimulated release of vIL-10 at both 30 min and 180 min, suggestive of a role for non-muscle Myo2 in its exocytosis. This effect was comparable to our previous observation that the CCH-stimulated release of the exogenous secretory product, syncollin-GFP, was also significantly reduced by ML-7 (Jerdeva et al., 2005a).

Myo5c is an unconventional myosin motor protein that is highly expressed in secretory epithelial cells from pancreas and lacrimal gland (Rodriguez and Cheney, 2002; Chen et al., 2006; Marchelletta et al., 2008). This protein is enriched in the subapical cytoplasm of lacrimal acini, in association with SV (Fig. 8B) (Marchelletta et al., 2008). Our previous work has shown extensive co-localization of Myo5c with the SV marker, rab3D. We have also shown that disruption of Myo5c activity through Ad-mediated expression of a dominant negative Myo5c-tail-GFP construct results in disruption of actin coat function during SV exocytosis and results in functional inhibition of exocytosis (Marchelletta et al., 2008). To test if Myo5c was functionally important in vIL-10 release, we used the dominant negative Myo5c-tail domain labeled with GFP inserted into an Ad expression vector (Ad-Myo5c-tail-GFP) to transduced LGAC. This construct functionally inhibits Myo5c activity, since the tail competes for cargo binding but the dominant negative construct is missing the head or motor domain and is therefore unable to transport the bound cargo along actin filaments (Rodriguez and Cheney, 2002). Ad-GFP was used as a control for Ad-Myo5c-tail-GFP in the dual transduction

experiments. Either construct was co-transduced with AdvIL-10 into LGAC. The transduction efficiencies of the Ad-Myo5c-tail-GFP and Ad-GFP constructs in LGAC, with or without AdvIL-10, were >80%, so essentially all vIL-10 expressing LGACs were co-transduced. As shown in Fig. 8A, co-transduction with Ad-Myo5c-tail-GFP significantly ($p \leq 0.05$) and substantially decreased CCH-stimulated vIL-10 secretion at 30 min and 180 min relative to cells doubly-transduced with AdvIL-10 and Ad-GFP.

Moreover, confocal fluorescence microscopy revealed that Ad-Myo5c-tail-GFP enhanced intracellular vIL-10 staining in AdvIL-10/Ad-Myo5c-tail-GFP-transduced cells stimulated by 100 μM CCH for 30 min compared to cells doubly-transduced with AdvIL-10 and Ad-GFP (Fig. 8C). Unlike the diffuse cytoplasmic GFP labeling from Ad-GFP transduction, Myo5c-tail-GFP was enriched largely in subapical compartments in LGAC. Considerable co-localization of vIL-10 and Myo5c-tail-GFP was also observed in the subapical region of resting acini doubly-transduced with AdvIL-10 and Ad-Myo5c-tail-GFP, while significantly more vIL-10 immunoreactivity was recovered in Myo5c-tail-GFP-positive subapical vesicular structures in doubly-transduced cells stimulated by 100 μM CCH for 30 min (Fig. 8C). These effects support a largely apical release mechanism for vIL-10 from LGAC which utilizes, at least in part, actin filaments, non-muscle Myo2 and Myo5c in ways previously implicated in SV exocytosis of other proteins.

4. Discussion

In this study, we have analyzed the intracellular trafficking and route of release of a therapeutic protein, vIL-10, introduced into LGAC using an adenoviral vector. Analysis of the intracellular routing and disposition of therapeutic proteins introduced by gene therapy is a critical element in evaluating their ultimate potential and efficacy. For instance, if a protein destined for secretion is introduced into the target cell but is not appropriately targeted to SV, this protein will not ultimately reach its target site. The problem becomes more complex when dealing with epithelial cells, which maintain distinct plasma membrane domains, apical and basolateral, facing different exteriors, in this case the ocular surface/tear film and the interstitium, respectively. Our study has demonstrated that vIL-10 immunoreactivity is associated with large apparent SV, indicating that it is appropriately packaged into membrane-bounded organelles. Analysis of the size of the vesicles, their intracellular locale and their co-localization with other markers of biosynthetic compartments suggests that vIL-10 is sorted primarily into apically-targeted SV. Observation that exposure of transduced LGAC to CCH elicited a burst of release of vIL-10 substantiates our hypothesis that these organelles are SV.

Our previous studies have demonstrated a dual role for actin filaments in exocytosis of SV (Jerdeva et al., 2005a). CCH stimulation is associated with the rapid and transient formation of actin coats around clusters of fusing SV that we have termed fusion intermediates. Inhibition of Myo5c or non-muscle Myo2 prevents the formation of actin-coated fusion intermediates or traps these structures at an intermediate stage in the subapical cytoplasm, while concomitantly reducing the amount of secretory proteins recovered in the extracellular fluid. By utilizing fluorescence recovery after photobleaching (FRAP) analysis, we have also shown that in addition to the assembly of actin coats around fusing vesicles that the actin network underlying the apical plasma membrane becomes much more dynamic (Jerdeva et al., 2005a). Disassembly of this actin barrier enhances the basal and CCH-stimulated release of SV proteins, suggesting a barrier role for this second population of actin filaments in exocytosis (Scheme 1), distinct from the actin coating on fusion intermediates. In the current study we have shown that the CCH-stimulated vIL-10 secretion from LGAC exhibits comparable sensitivity to LAT treatment relative to syncollin-GFP, an SV marker (Jerdeva et al., 2005a), suggesting that secretion of vIL-10 is optimal when the actin barrier is transiently removed. As well, relative to syncollin-GFP (Jerdeva et al., 2005a), CCH-stimulated vIL-10 secretion from LGAC

exhibits comparable sensitivity to ML-7 treatment and dominant negative Myo5c overexpression, suggesting that optimal secretion of vIL-10 requires the activity of both of these myosin motors. Finally, vIL-10 immunofluorescence is co-localized with that from Myo5c-tail-GFP which has been previously shown to associate with SV (Marchelletta et al., 2008). Each of these responses is characteristic of the behavior of other secretory or tear proteins in LGAC; therefore we propose that most vIL-10 is routed through a specific SV population at the apical plasma membrane.

Since the maintenance of prolonged secretory responses of some secretory proteins are dependent upon the continued trafficking of materials along cellular microtubules to produce new SV, it was somewhat surprising that we detected no inhibitory effects of the microtubule-destabilizing agent, nocodazole, on CCH-stimulated vIL-10 release. However, our explorations of the role of the microtubule array in rSV maturation and exocytosis have focused only on β-hexosaminidase and bulk protein. As is shown in Fig. 5, the acute release kinetics of β-hexosaminidase differ from those of vIL-10, suggesting that they may be packaged in distinct SV. Interestingly, inhibition of Myo5c does not impair CCH-stimulated β-hexosaminidase release, although it inhibits the CCH-stimulated release of syncollin-GFP (Marchelletta et al., 2008). Ample evidence exists for the existence of multiple SV types in LGAC, ranging from the observation of vesicles that exhibit different electron densities consistent with different contents (da Costa et al., 2006), to the observation that different SV markers such as syncollin-GFP, β-hexosaminidase and now vIL-10 exhibit subtly different acute release kinetics. By extension, the pathways involved in the production of different rSV in LGAC may not be equally dependent upon the microtubule array.

In conclusion, here we have demonstrated that a transduced protein can be delivered and released primarily through apical exocytosis from SV in an actin- and myosin-dependent manner in LGAC. This has important ramifications for our understanding of the therapeutic mechanisms of action of transduced vIL-10 in the rabbit model of autoimmune dacryoadenitis. This also suggests that the LGAC can be engineered, not only for regulated release of therapeutic proteins for diseases of the lacrimal gland, but that it can be targeted more broadly as a reservoir that can sustain the regulated release of therapeutic proteins which, when released into tear fluid, can treat disorders of the cornea and even the posterior segment.

Acknowledgements

This study was supported by NIH grants EY012689 (MDT), EY011386 (SHA), EY017293 (SHA), EY016985 (SHA) and DC03299 (REC). DTJ was supported by a Porter Fellowship from the American Physiological Society and an UNC Sequoyah Dissertation Fellowship. The authors thank members of Dr. Sarah Hamm-Alvarez's lab for their help conducting this work.

Abbreviations

KCS, keratoconjunctivitis sicca
SjS, Sjögren's syndrome
vIL-10, viral interleukin-10
SV, secretory vesicle(s)
rSV, recruitable secretory vesicle(s)
LGAC, lacrimal gland acinar cell
CCH, carbachol
Ad5, adenovirus serotype 5
AdvIL-10, adenovirus serotype 5 containing viral interleukin-10
Myo5c, myosin 5c
Myo2, myosin 2
Ad-GFP, adenovirus serotype 5 containing green fluorescent protein

Ad-Myo5c-tail-GFP, adenovirus serotype 5 containing the GFP-fused tail region of myosin 5c
LAT, latrunculin B
EEA1, early endosomal antigen 1
MOI, multiplicity of infection
DPBS, Dulbecco's phosphate buffered saline

References

Andersson SV, Edman MC, Bekmezian A, Holmberg J, Mircheff AK, Gierow JP. Characterization of beta-hexosaminidase secretion in rabbit lacrimal gland. Exp. Eye Res 2006;83:1081–1088. [PubMed: 16839547]

Chen X, Walker AK, Strahler JR, Simon ES, Tomanicek-Volk SL, Nelson BB, Hurley MC, Ernst SA, Williams JA, Andrews PC. Organellar proteomics: analysis of pancreatic zymogen granule membranes. Mol. Cell. Proteomics 2006;5:306–312. [PubMed: 16278343]

Crystal RG. Transfer of genes to humans: early lessons and obstacles to success. Science 1995;270:404–410. [PubMed: 7569994]

da Costa SR, Sou E, Xie J, Yarber FA, Okamoto CT, Pidgeon M, Kessels MM, Mircheff AK, Schechter JE, Qualmann B, Hamm-Alvarez SF. Impairing actin filament or syndapin functions promotes accumulation of clathrincoated vesicles at the apical plasma membrane of acinar epithelial cells. Mol. Biol. Cell 2003;14:4397–4413. [PubMed: 12937279]

da Costa SR, Wu K, MacVeigh M, Pidgeon M, Ding C, Schechter JE, Hamm-Alvarez SF. Male NOD mouse external lacrimal glands exhibit profound changes in the exocytotic pathway early in postnatal development. Exp. Eye Res 2006;82:33–45. [PubMed: 16005870]

da Costa SR, Yarber FA, Zhang L, Sonee M, Hamm-Alvarez SF. Microtubules facilitate the stimulated secretion of beta-hexosaminidase in lacrimal acinar cells. J. Cell Sci 1998;111:1267–1276. [PubMed: 9547304]

Evans CH, Whalen JD, Ghivizzani SC, Robbins PD. Gene therapy in autoimmune diseases. Ann. Rheum. Dis 1998;57:125–127. [PubMed: 9640124]

Fox RI. Sjogren's syndrome: current therapies remain inadequate for a common disease. Expert Opin. Investig. Drugs 2000;9:2007–2016.

Gierow JP, Lambert RW, Mircheff AK. Fluid phase endocytosis by isolated rabbit lacrimal gland acinar cells. Exp. Eye Res 1995;60:511–525. [PubMed: 7615017]

Goldfine ID, German MS, Tseng HC, Wang J, Bolaffi JL, Chen JW, Olson DC, Rothman SS. The endocrine secretion of human insulin and growth hormone by exocrine glands of the gastrointestinal tract. Nat. Biotechnol 1997;15:1378–1382. [PubMed: 9415890]

Hamm-Alvarez SF, da Costa S, Yang T, Wei X, Gierow JP, Mircheff AK. Cholinergic stimulation of lacrimal acinar cells promotes redistribution of membrane-associated kinesin and the secretory protein, β-hexosaminidase, and increases kinesin motor activity. Exp. Eye Res 1997;64:141–156. [PubMed: 9176047]

Hamm-Alvarez SF, Xie J, Wang Y, Medina-Kauwe LK. Modulation of secretory functions in epithelia by adenovirus capsid proteins. J. Control. Release 2003;93:129–140. [PubMed: 14636719]

Jerdeva GV, Wu K, Yarber FA, Rhodes CJ, Kalman D, Schechter JE, Hamm-Alvarez SF. Actinandnon-musclemyosinIIfacilitateapicalexocytosisoftear proteinsin rabbitlacrimalacinarepithelial cells. J.CellSci 2005a;118:4797–4812.

Jerdeva GV, Yarber FA, Trousdale MD, Rhodes CJ, Okamoto CT, Dartt DA, Hamm-Alvarez SF. Dominant-negative PKC-epsilon impairs apical actin remodeling in parallel with inhibition of carbachol-stimulated secretion in rabbit lacrimal acini. Am. J. Physiol. Cell Physiol 2005b; 289:C1052–C1068. [PubMed: 15930141]

Lemp MA. Dry eye (keratoconjunctivitis sicca), rheumatoid arthritis, and Sjogren's syndrome. Am. J. Ophthalmol 2005;140:898–899. [PubMed: 16310468]

Lever, AM.; Goodfellow, P. Gene Therapy. Churchill Livingstone; New York, NY: 1995. p. 1-91.

Marchelletta RR, Jacobs DT, Schechter JE, Cheney RE, Hamm-Alvarez SF. The class V myosin motor, myosin 5c, localizes to mature secretory vesicles and facilitates exocytosis in lacrimal acini. Am. J. Physiol. Cell Physiol 2008;295:C13–C28. [PubMed: 18434623]

Mathisen PM, Tuohy VK. Gene therapy in the treatment of autoimmune disease. Immunol. Today 1998;19:103–105. [PubMed: 9540266]

Mircheff AK, Wang Y, Jean Mde S, Ding C, Trousdale MD, Hamm-Alvarez SF, Schechter JE. Mucosal immunity and self-tolerance in the ocular surface system. Ocul. Surf 2005;3:182–192. [PubMed: 17131026]

Pflugfelder SC, Solomon A, Stern ME. The diagnosis and management of dry eye: a twenty-five-year review. Cornea 2000;19:644–649. [PubMed: 11009316]

Rodriguez OC, Cheney R. Human myosin-Vc is a novel class V myosin expressed in epithelial cells. J. Cell Sci 2002;115:991–1004. [PubMed: 11870218]

Saitoh M, Ishikawa T, Matsushima S, Naka M, Hidaka H. Selective inhibition of catalytic activity of smooth muscle myosin light chain kinase. J. Biol. Chem 1987;262:7796–7801. [PubMed: 3108259]

Schaumberg DA, Sullivan DA, Buring JE, Dana MR. Prevalence of dry eye syndrome among US women. Am. J. Ophthalmol 2003;136:318–326. [PubMed: 12888056]

Segerberg-Konttinen M. Focal adenitis in lacrimal and salivary glands. A post-mortem study. Scand. J. Rheumatol 1988;17:379–385. [PubMed: 3212408]

Seroogy CM, Fathman CG. A gene therapy approach to treatment of autoimmune disease. Immunol. Res 1998;18:15–26. [PubMed: 9724846]

Trousdale MD, Zhu Z, Stevenson D, Schechter JE, Ritter T, Mircheff AK. Expression of TNF inhibitor gene in the lacrimal gland promotes recovery of tear production and tear stability and reduced immunopathology in rabbits with induced autoimmune dacryoadenitis. J. Autoimmune Dis 2005;28:2–6.

Wang Y, Jerdeva G, Yarber FA, da Costa SR, Xie J, Qian L, Rose CM, Mazurek C, Kasahara N, Mircheff AK, Hamm-Alvarez SF. Cytoplasmic dynein participates in apically targeted stimulated secretory traffic in primary rabbit lacrimal acinar epithelial cells. J. Cell Sci 2003;116:2051–2065. [PubMed: 12679381]

Wang Y, Xie J, Yarber FA, Mazurek C, Trousdale MD, Medina-Kauwe LK, Kasahara N, Hamm-Alvarez SF. Adenoviral capsid modulates secretory compartment organization and function in acinar epithelial cells from rabbit lacrimal acini. Gene Ther 2004;11:970–981. [PubMed: 15029229]

Wu K, Jerdeva GV, da Costa SR, Sou E, Schechter JE, Hamm-Alvarez SF. Molecular mechanisms of lacrimal acinar secretory vesicle exocytosis. Exp. Eye Res 2006;83:84–96. [PubMed: 16530759]

Xie J, Chiang L, Contreras J, Wu K, Garner JA, Medina-Kauwe L, Hamm-Alvarez SF. Novel fiber-dependent entry mechanism for adenovirus serotype 5 in lacrimal acini. J. Virol 2006;80:11833–11851. [PubMed: 16987972]

Xie J, Qian L, Wang Y, Hamm-Alvarez SF, Mircheff AK. Role of the microtubule cytoskeleton in traffic of EGF through the lacrimal acinar cell endomembrane network. Exp. Eye Res 2004a;78:1093–1106. [PubMed: 15109916]

Xie J, Qian L, Wang Y, Rose CM, Yang T, Nakamura T, Hamm-Alvarez SF, Mircheff AK. Novel biphasic traffic of endocytosed EGF to recycling and degradative compartments in lacrimal gland acinar cells. J. Cell. Physiol 2004b;199:108–125. [PubMed: 14978740]

Zhang L, da Costa SR, Yarber FA, Runnegar M, Hamm-Alvarez SF. Protein phosphatase inhibitors alter cellular microtubules and reduce carbachol-dependent protein secretion in lacrimal acini. Curr. Eye Res 2000;20:373–383. [PubMed: 10855032]

Zhu Z, Stevenson D, Ritter T, Schechter JE, Mircheff AK, Kaslow HR, Trousdale MD. Expression of IL-10 and TNF-inhibitor genes in lacrimal gland epithelial cells suppresses their ability to activate lymphocytes. Cornea 2002;21:210–214. [PubMed: 11862098]

Zhu Z, Stevenson D, Schechter JE, Mircheff AK, Atkinson R, Trousdale MD. Lacrimal histopathology and ocular surface disease in a rabbit model of autoimmune dacryoadenitis. Cornea 2003a;22:25–32. [PubMed: 12502944]

Zhu Z, Stevenson D, Schechter JE, Mircheff AK, Crow RW, Atkinson R, Ritter T, Bose S, Trousdale MD. Tumor necrosis factor inhibitor gene expression suppresses lacrimal gland immunopathology in a rabbit model of autoimmune dacryoadenitis. Cornea 2003b;22:343–351. [PubMed: 12792478]

Zhu Z, Stevenson D, Schechter JE, Mircheff AK, Ritter T, Labree L, Trousdale MD. Prophylactic effect of IL-10 gene transfer on induced autoimmune dacryoadenitis. Investig. Ophthalmol. Vis. Sci 2004;45:1375–1381. [PubMed: 15111591]

Zoukhri D. Effect of inflammation on lacrimal gland function. Exp. Eye Res 2006;82:885–898. [PubMed: 16309672]

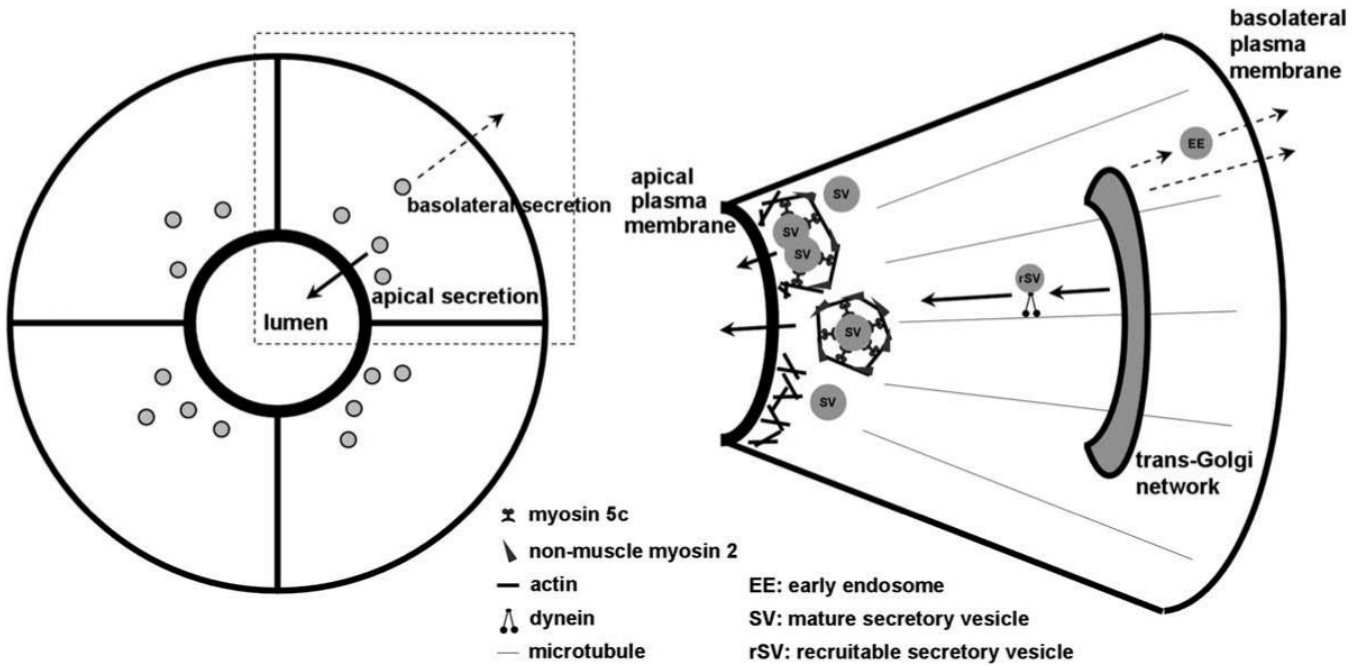

Scheme 1.

The diagram to the left depicts individual lacrimal acinar cells organized around a central lumenal region, as well as the directions for apical and basolateral secretion of proteins from the cell. The apical plasma membrane domain can be distinguished in intact tissue and in the in vitro reconstituted cultures by the intense labeling associated with the subapical actin filament network. The diagram to the right depicts a single acinar cell expanded from the panel to the left. SV are shown concentrated in the subapical cytoplasm beneath the actin-enriched apical plasma membrane. Some SV are undergoing fusion, by being enveloped in actin coats enriched in non-muscle Myo2 and Myo5c, adjacent to spots where actin filaments have transiently disassembled beneath the apical plasma membrane. Exocytosis using these mechanisms is elicited by secretagogue stimulation (bold arrows). rSV are also shown moving towards the apical plasma membrane to sustain the secretory response, a response evoked by secretagogue stimulation (bold arrows). Other vesicular traffic emerging from the trans-Golgi network can be sorted to the basolateral membrane for constitutive exocytosis (dashed arrows).

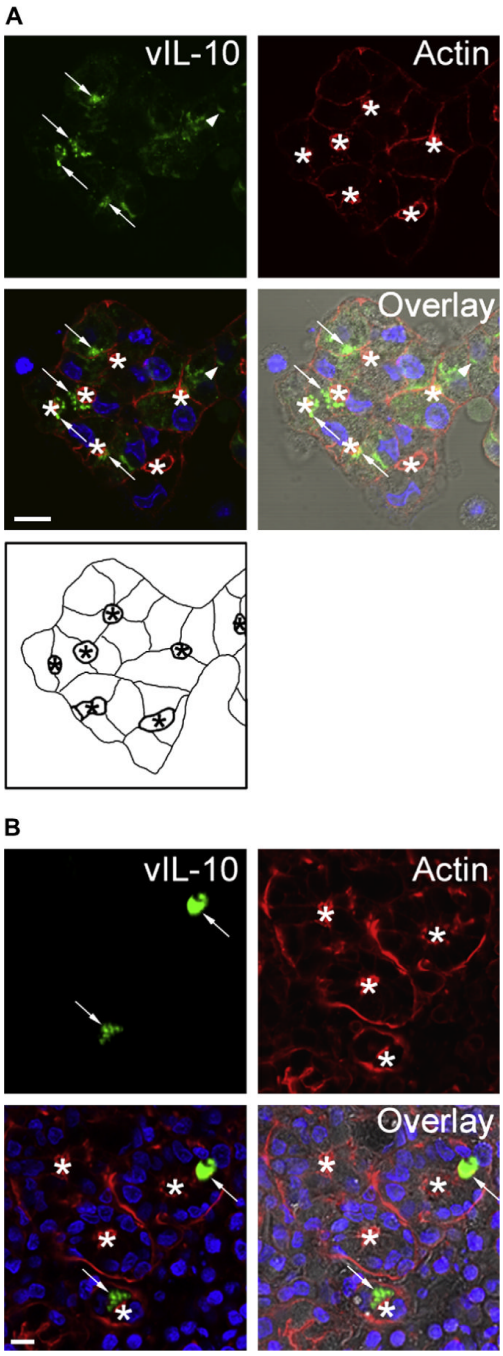

Fig. 1.

vIL-10 immunoreactivity is detected in large intracellular vesicles in transduced LGAC. A. Rabbit LGACs were seeded onto Matrigel-coated 18 mm circular glass coverslips in 12-well plates at 2×10^6 cells/well. On day 2 of culture, reconstituted acini were transduced with AdvIL-10 at a MOI of 5 for 24 h. Cells were then fixed and processed to fluorescently label vIL-10 (green), actin filaments (red) and cellular nuclei (blue). The DIC image is also shown for comparison. Arrows, accumulation of vIL-10 in large vesicles beneath the actin-enriched apical plasma membrane; arrowhead, accumulation of vIL-10 in basolateral structures; bar, 10 μm and *, apical/lumenal region. A schematic diagram of the acini transduced with AdvIL-10 is also shown for reference. The lumen (indicated with an asterisk) is bounded by the apical

plasma membranes (thick lines). Basolateral plasma membranes are illustrated as thinner lines. B. Immunocytochemistry studies of IL-10 expression at 5 days post-injection in rabbit inferior lacrimal glands. AdvIL-10 (1×10^8 PFU in 0.2 mL) was injected into each rabbit's inferior lacrimal gland as described in Section 2. 5 days after inoculation, rabbits were sacrificed and inferior lacrimal glands were removed from each animal. After fixing in 4% paraformaldehyde and sucrose rehydration, the glands were embedded in OCT and frozen sections were processed to fluorescently label vIL-10 (green), actin filaments (red) and cellular nuclei (blue). The DIC image is also shown for comparison. Arrows, accumulation of vIL-10 in vesicle-like structures beneath the apical plasma membrane; bar, 10 μm and *, apical/lumenal region.

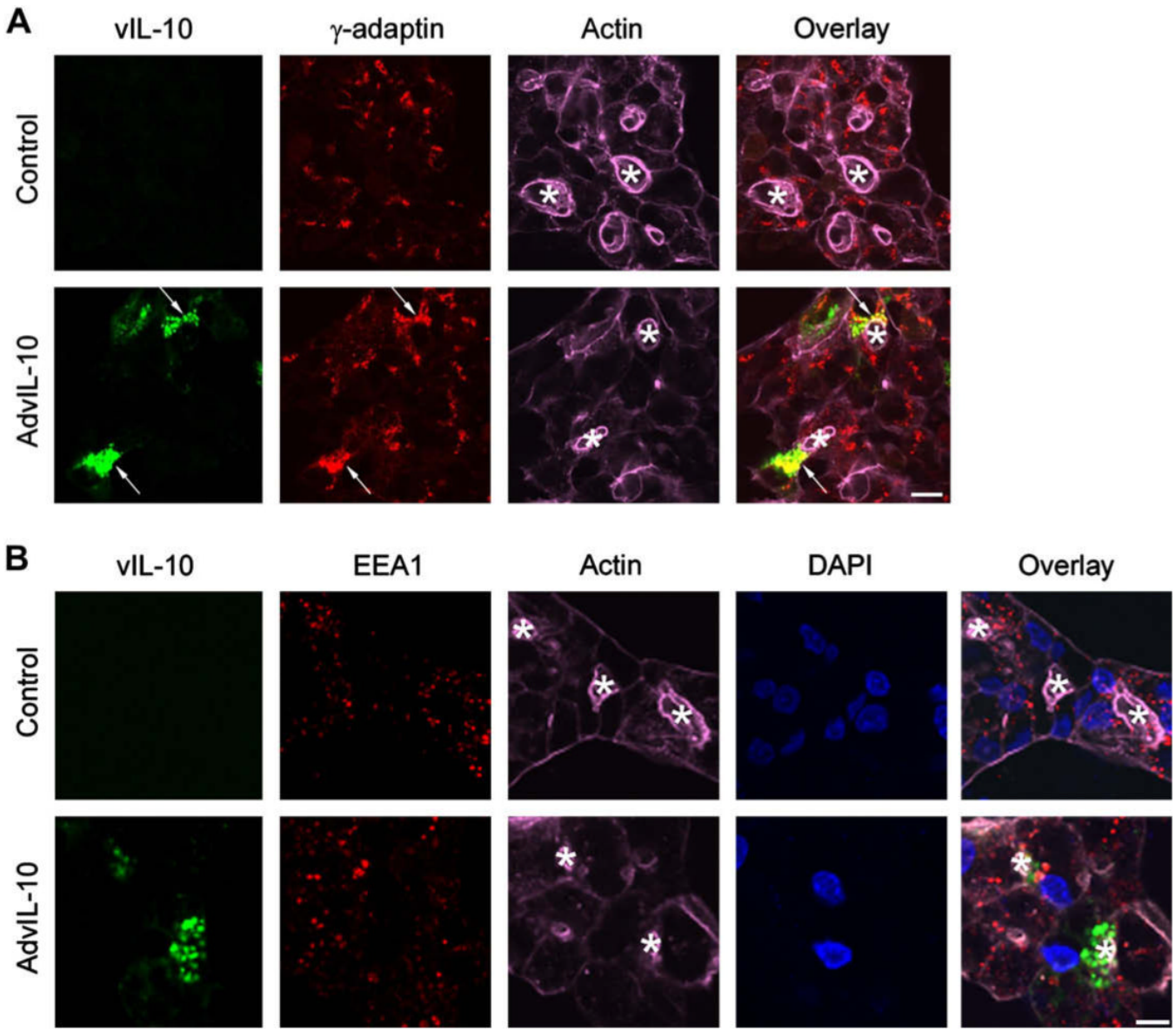

Fig. 2.

vIL-10 is partially co-localized with biosynthetic but not basolateral endosomal markers. Rabbit LGACs were cultured and transduced with AdvIL-10 as described in legend for Fig. 1A. Cells were then fixed and processed to fluorescently label vIL-10 (green), γ-adaptin (A) or EEA1 (B) (red), actin filaments (purple) and DAPI (blue). Arrows, co-localization of vIL-10 and γ-adaptin; bar, 10 μm and *, apical/lumenal region.

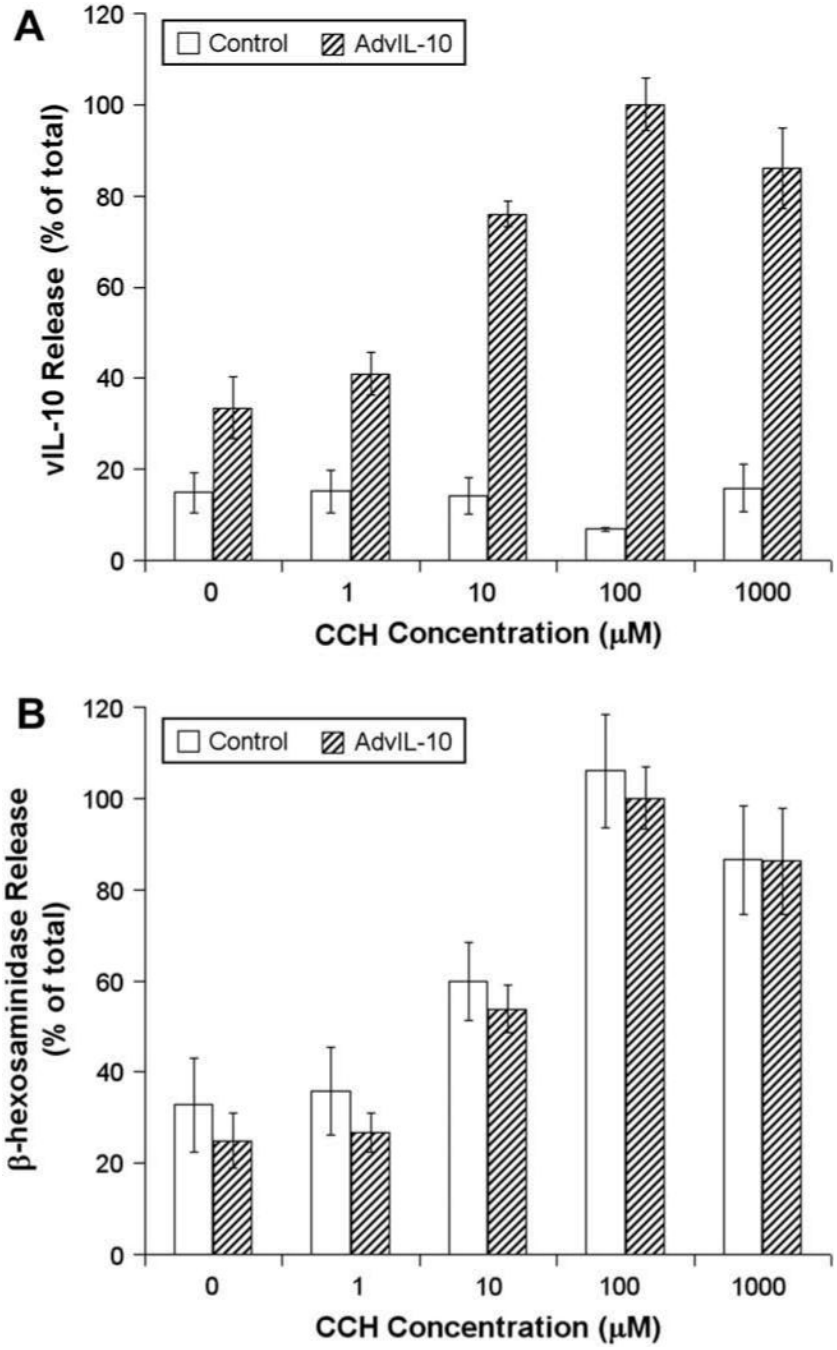

Fig. 3.

Dose dependence of CCH-stimulated release of vIL-10 and β-hexosaminidase from LGAC. Rabbit LGACs were seeded onto Matrigel-coated 24-well plates at 1×10^6 cells/well. On day 2 of culture, reconstituted acini were transduced with AdvIL-10 at a MOI of 5 for 24 h. Control and transduced acini were then incubated in fresh medium for 1 h to allow cell equilibration. After treatment without or with 1, 10, 100 and 1000 μM CCH for 30 min, aliquots of the medium were collected and processed for measurement of vIL-10 (A) and β-hexosaminidase (B) release using ELISA and biochemical assays, respectively. vIL-10 and β-hexosaminidase release are plotted as % of total, with total defined as the maximal release elicited by 100 μM CCH at 30 min in acini transduced with AdvIL-10. $n = 4$. Error bars represent s.e.m.

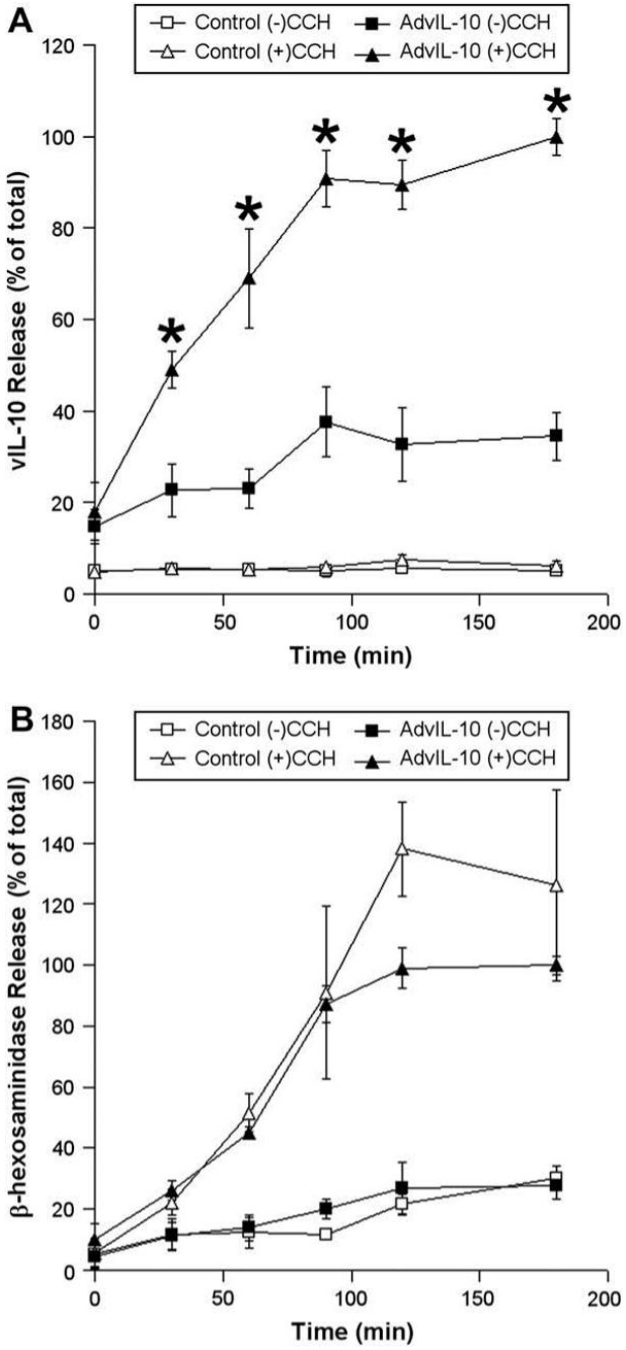

Fig. 4.

Time course of CCH-stimulated release of vIL-10 and β-hexosaminidase from LGAC. Rabbit LGACs were cultured and transduced with AdvIL-10 as described in the legend for Fig. 3. After treatment with or without 100 μM CCH at time intervals from 0 to 180 min, aliquots of the medium were collected and processed for measurement of vIL-10 (A) and β-hexosaminidase (B) release using ELISA and biochemical assays, respectively. vIL-10 and β-hexosaminidase release are plotted as % of total, with total defined as the maximal release elicited by 100 μM CCH at 180 min. $n = 3$ and *, significant at $p \leq 0.05$, AdvIL-10 (+)CCH versus AdvIL-10 (−)CCH. Error bars represent s.e.m.

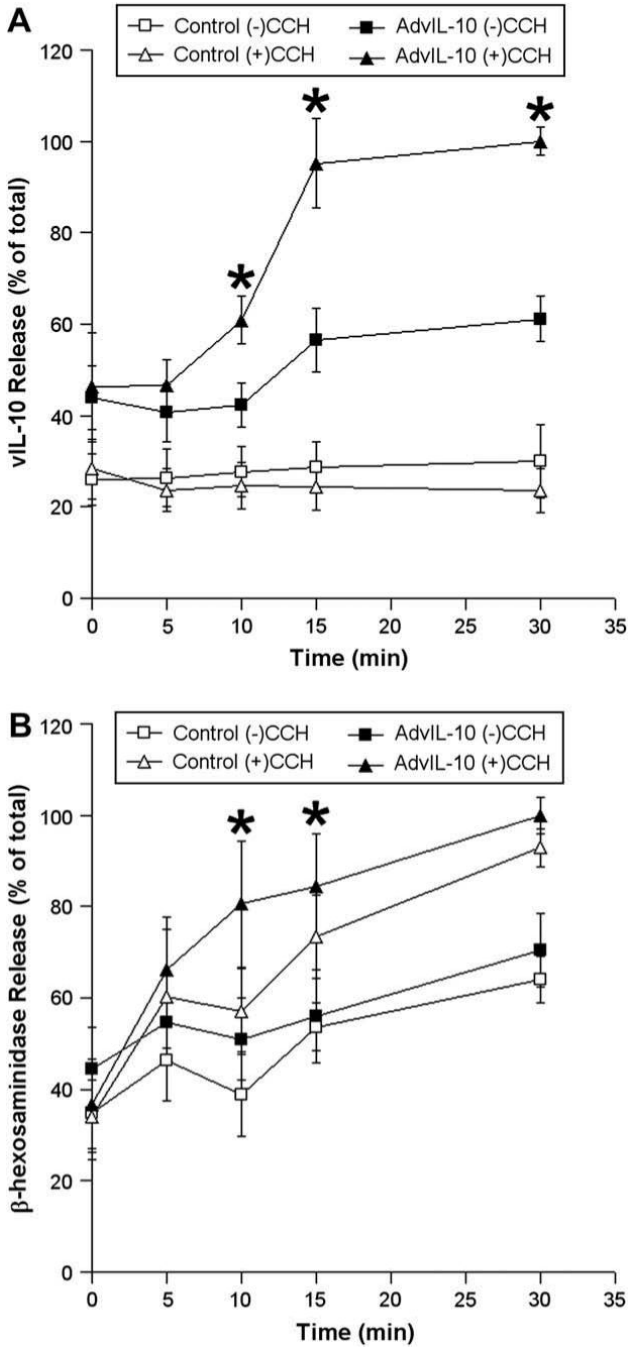

Fig. 5.

Acute release of vIL-10 and β-hexosaminidase from LGAC. Rabbit LGACs were cultured and transduced with AdvIL-10 as described in the legend for Fig. 3. After treatment with or without 100 μM CCH at time intervals from 0 to 30 min, aliquots of the medium were collected and processed for measurement of vIL-10 (A) and β-hexosaminidase (B) release using ELISA and biochemical assays, respectively. vIL-10 and β-hexosaminidase release are plotted as % of total, with total defined as the maximal release elicited by 100 μM CCH at 30 min. $n = 5$ and *, significant at $p \leq 0.05$, AdvIL-10 (+)CCH versus AdvIL-10 (−)CCH (A) and AdvIL-10 (+)CCH versus Control (+)CCH (B). Error bars represent s.e.m.

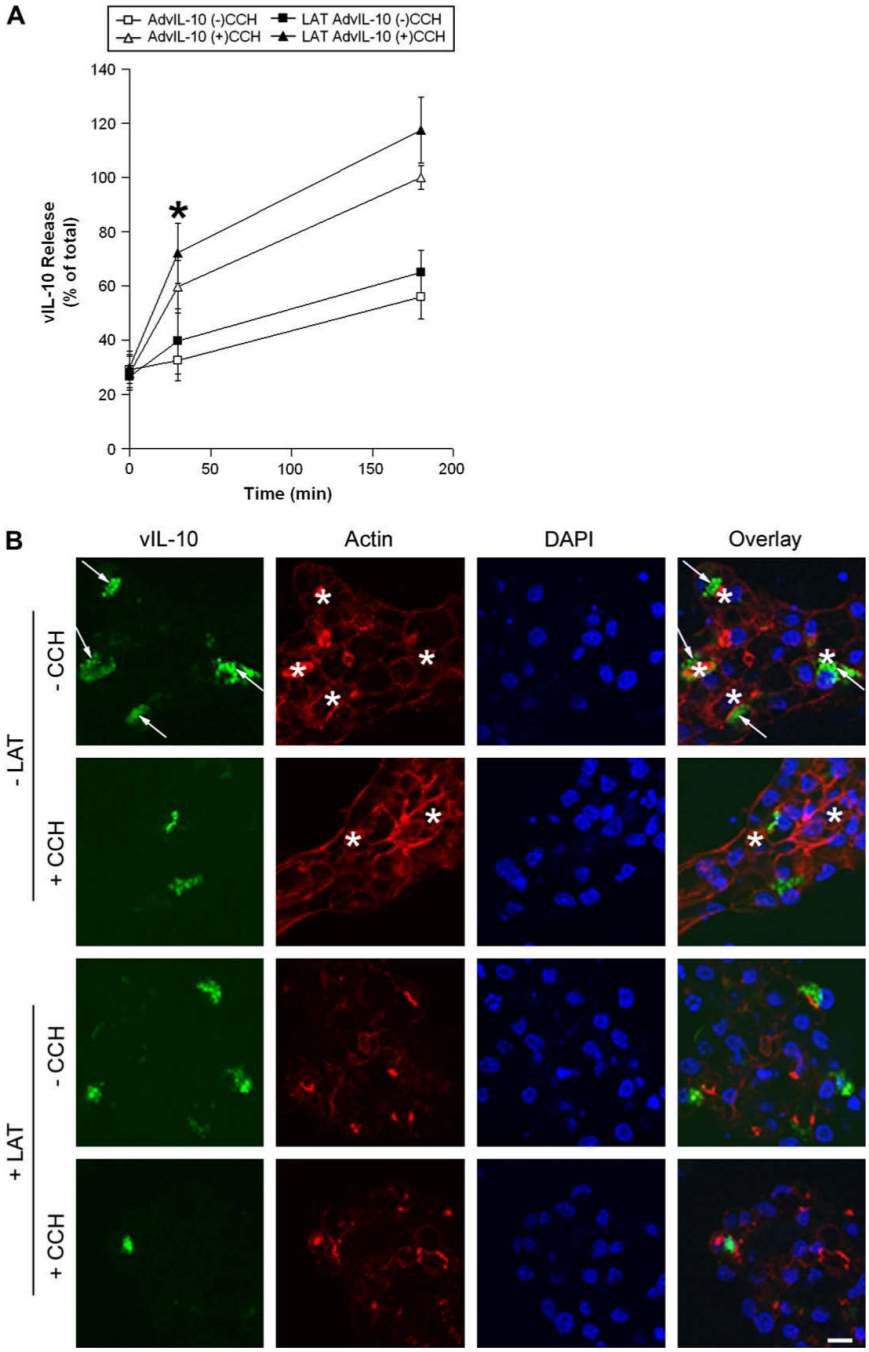

Fig. 6.

Disruption of actin filaments modulates vIL-10 secretion from LGAC. A. Effect of latrunculin B (LAT) pretreatment on CCH-stimulated release of vIL-10 from LGAC. Rabbit LGACs were cultured and transduced with AdvIL-10 as described in legend for Fig. 3. Cells were then pretreated with LAT (10 μM) for 60 min before being treated without or with 100 μM CCH at time intervals from 0 to 180 min. Aliquots of the medium were collected and processed for measurement of vIL-10 release using ELISA assays. vIL-10 release is plotted as % of total, with total defined as the maximal release elicited by 100 μM CCH at 180 min in untreated cells. $n = 5$ and *, significant at $p \leq 0.05$, LAT AdvIL-10 (+)CCH versus AdvIL-10 (+)CCH. Error bars represent s.e.m. B. Effect of LAT pretreatment on vIL-10 distribution in LGAC.

Rabbit LGACs were cultured and transduced with AdvIL-10 as described in legend for Fig. 1A. Cells were then pretreated with LAT (10 μM) for 60 min before being treated without or with 100 μM CCH for 30 min. Cells were fixed and processed to fluorescently label vIL-10 (green), actin filaments (red) and cellular nuclei (blue). Arrows, subapical accumulation of vIL-10; bar, 10 μm and *, apical/lumenal region.

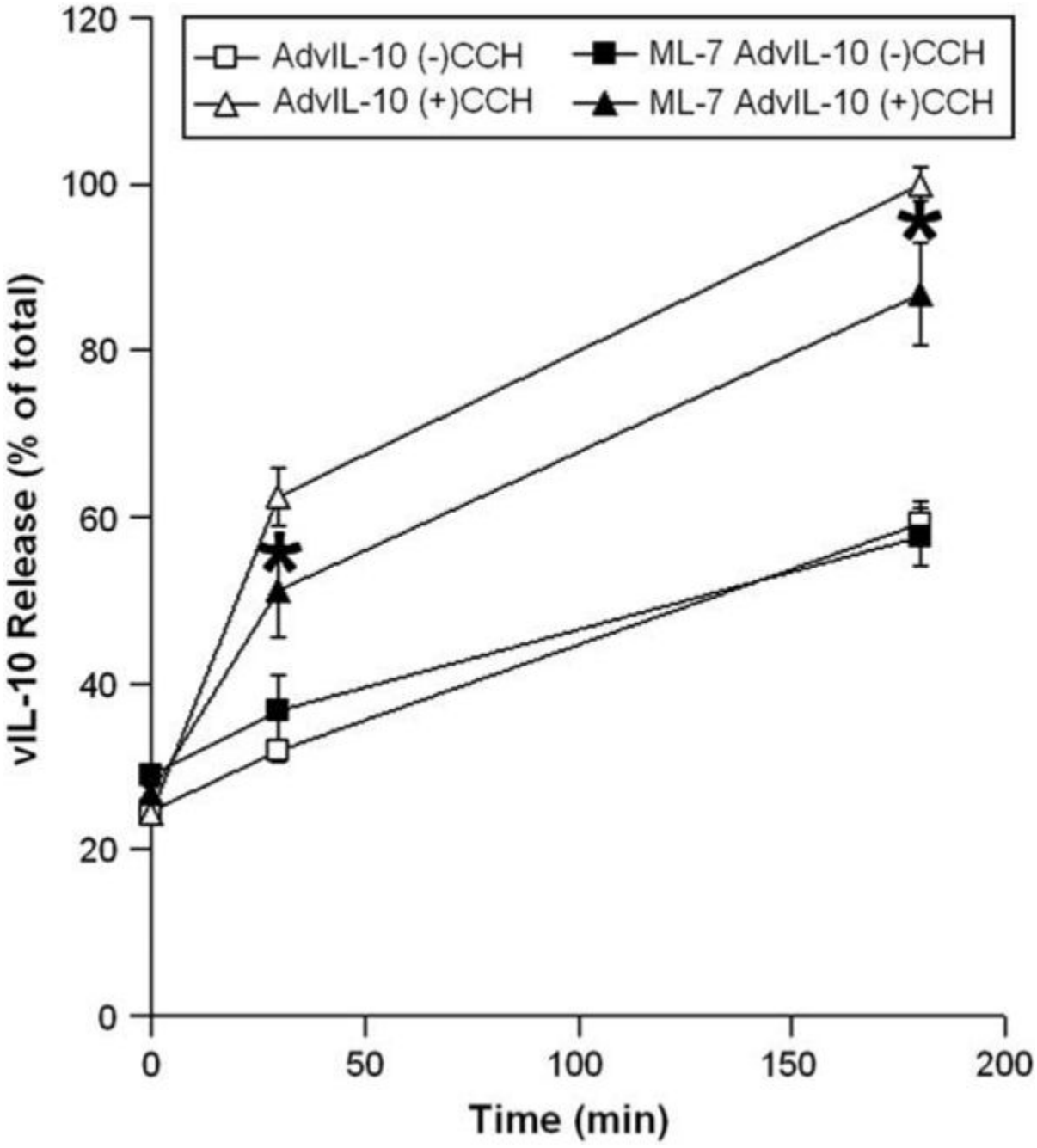

Fig. 7.

Myosin motors participate in vIL-10 secretion from LGAC. Rabbit LGACs were cultured and transduced with AdvIL-10 as described in legend for Fig. 3. Cells were then pretreated with the non-muscle Myo2 inhibitor, ML-7 (40 μM), for 15 min before being treated without or with 100 μM CCH at time intervals from 0 to 180 min. Aliquots of the medium were collected and processed for measurement of vIL-10 release using ELISA. vIL-10 release is plotted as % of total, with total defined as the maximal release elicited by 100 μM CCH at 180 min in untreated acini. $n = 8$ and *, significant at $p \leq 0.05$, ML-7 AdvIL-10 (+)CCH versus AdvIL-10 (+)CCH. Error bars represent s.e.m.

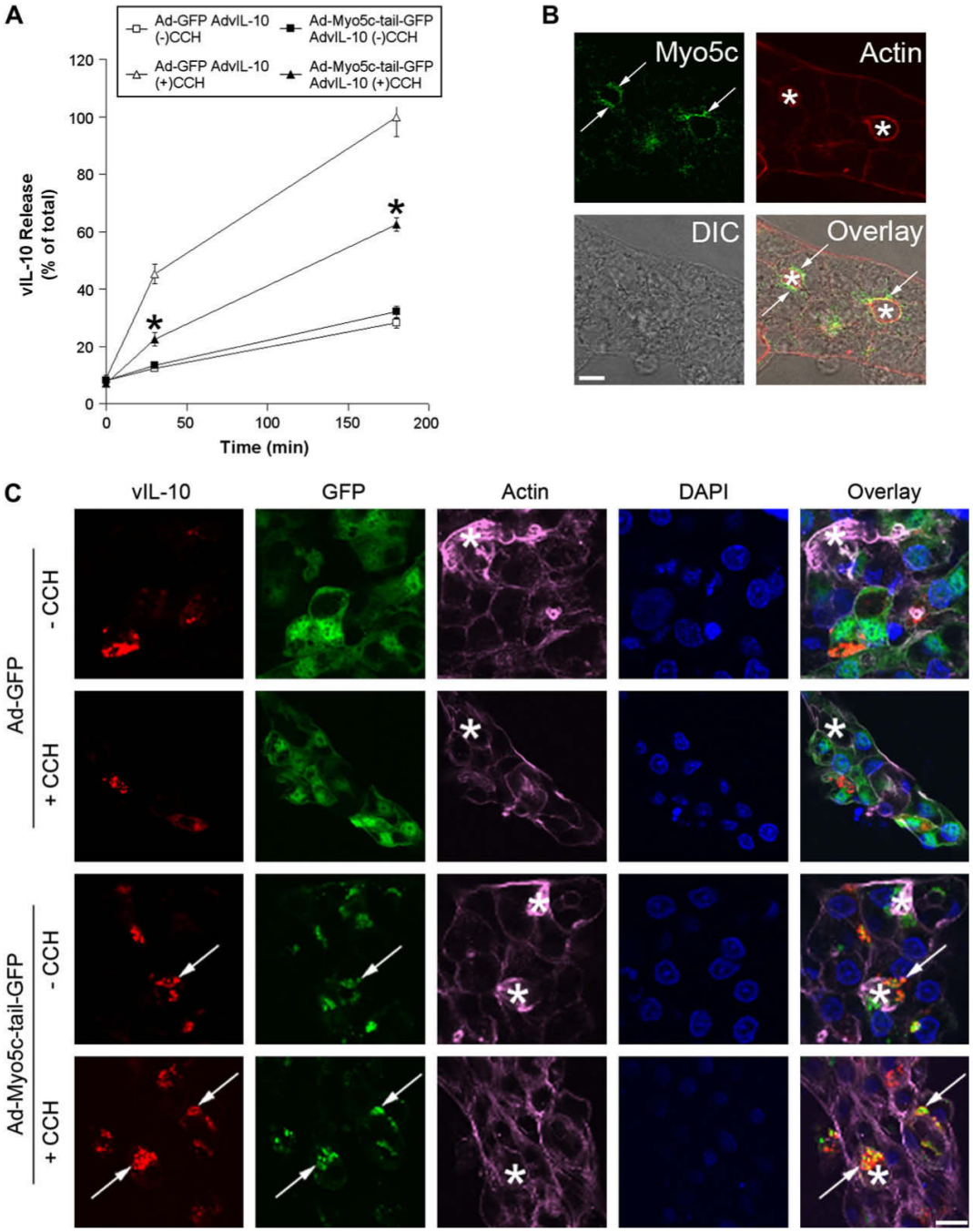

Fig. 8.

Myosin 5c participates in vIL-10 secretion from LGAC. A. Effect of Ad-Myo5c-tail-GFP transduction on CCH-stimulated release of vIL-10 from LGAC. Rabbit LGACs were seeded onto Matrigel-coated 24-well plates at 1×10^6 cells/well. On day 2 of culture, reconstituted acini were singly or doubly-transduced with Ad-GFP, Ad-Myo5c-tail-GFP or AdvIL-10 at a MOI of 5 for 24 h. Control and transduced acini were then incubated in fresh medium for 1 h to allow cell equilibration. After treatment with or without 100 μM CCH at time intervals from 0 to 180 min, aliquots of the medium were collected and processed for measurement of vIL-10 release using ELISA assays. vIL-10 release is plotted as % of total, with total defined as the maximal release elicited by 100 μM CCH at 180 min in acini doubly-transduced with AdvIL-10

and Ad-GFP. $n = 10$ and *, significant at $p \leq 0.05$, Ad-Myo5c-tail-GFP AdvIL-10 (+)CCH versus Ad-GFP AdvIL-10 (+)CCH. Error bars represent s.e.m. B. Rabbit LGACs were seeded onto Matrigel-coated 18 mm circular glass coverslips in 12-well plates at 2×10^6 cells/well. On day 3 of culture, reconstituted acini were fixed and processed to fluorescently label Myo5c (green) and actin filaments (red). The DIC image is shown for comparison and the overlay image shows the super-imposition of the fluorescence image and the DIC image. Arrows, large apparent SV enriched in Myo5c; bar, 5 μm and *, apical/lumenal region. C. Effect of Ad-Myo5c-tail-GFP transduction on vIL-10 distribution in LGAC. Rabbit LGACs were seeded onto Matrigel-coated 12-well plates at 2×10^6 cells/well. On day 2 of culture, reconstituted acini were singly or doubly-transduced with Ad-GFP, Ad-Myo5c-tail-GFP or AdvIL-10 at a MOI of 5 for 24 h. Cells were then fixed and processed to fluorescently label vIL-10 (red), GFP (green), actin filaments (purple) and cellular nuclei (blue). Arrows, co-localization of vIL-10 and Myo5c-tail-GFP; bar, 10 μm and *, apical/lumenal region.